Near-trench coupling conditions offshore the Nicoya Peninsula, Costa Rica and Southern Nicaragua

M. S. Hastings[1], E. O. Lindsey[2], T. H. Dixon[1], S. Xie[3]

[1]University of South Florida, School of Geosciences
[2]University of New Mexico, Earth & Planetary Sciences
[3]University of Houston, Department of Civil and Environmental Engineering

Key Points:

- Large earthquakes occur offshore Nicaragua and generate tsunamis; similar size earthquakes in northern Costa Rica do not.
- Stress-constrained coupling models for Costa Rica suggest some shallow locking; Seismicity and GPS data in Nicaragua suggest shallow locking is possible.
- Sea-floor geodesy is necessary to better constrain conditions on the shallow megathrust in both regions.

Corresponding author: Mitchell Hastings, `mshastings1@usf.edu`

Abstract

Subduction zone tsunamis require significant co-seismic slip in the shallow, offshore plate interface near the trench, possibly related to the degree of prior interseismic coupling. In Nicaragua, a large tsunami was associated with the 1992 M_w 7.7 earthquake. To the south, the 2012 M_w 7.6 earthquake in the Nicoya peninsula of Costa Rica did not generate a tsunami. The disparate behavior between these two adjacent segments of the Central American megathrust remains unexplained. A stress-constrained model of slip deficit applied to the interseismic surface velocity field in Nicoya suggests a slip deficit rate in the updip portion of the megathrust between $0.8 - 8.5\,\mathrm{cm/yr}$, suggesting that large tsunamis are possible here. Limited GPS data in Nicaragua can be reconciled by an offshore locked zone that matches the shallow rupture model of the 1992 tsunami. Seafloor geodesy would allow much better near-trench constraints on slip deficit in both regions.

Plain Language Summary

Places where an oceanic plate converges and dives below another plate (continental or oceanic) host the largest earthquakes on Earth. Some but not all of these earthquakes cause catastrophic tsunamis. In the time between earthquakes, part of the sloping boundary between the two plates (the plate interface) is 'stuck,' deforming the Earth's crust. This deformation can be measured at the surface and used to infer motion on the interface. Along the western coast of Central America, the Cocos plate dives beneath the Caribbean plate. The region experiences frequent large earthquakes. Occasional tsunamis occur offshore Nicaragua but not Costa Rica. We use GPS data in the two regions to estimate the amount of motion on the shallow interface close to the sea floor. The data suggest that tsunamis represent a future hazard to both regions.

1 Introduction

One of the challenges in subduction zone hazard assessment is understanding whether a large or great earthquake will be accompanied by a catastrophic tsunami. Attempts have been made to investigate shallow, up-dip locking near the trench using existing on-land GPS, however, they have been unable to determine if that region is fully coupled or freely slipping (Schmalzle et al., 2014; Li et al., 2018). Sea-floor geodetics such as absolute pressure gauges (APGs) and GPS-acoustic (GPS-A) systems have made substantial strides in identifying and constraining shallow locking, but are expensive and difficult to implement and interpret (Bürgmann & Chadwell, 2014; Wallace et al., 2016; Yokota et al., 2016).

The Cocos plate subducts beneath the Caribbean plate at a rate of ~ 84 mm/yr with slight obliquity (DeMets, 2001; DeMets et al., 2010). Historically, the resulting subduction zone offshore Central America has hosted frequent M $\sim 7.2-7.8$ earthquakes with relatively short recurrence intervals, less than 100 years (Figure 1) (Satake, 1994; Protti et al., 1995). Slow slip events (SSEs) are also known here, releasing some fraction of accumulated strain in an aseismic or weakly seismic manner, often accompanied by low frequency earthquakes and non-volcanic seismic tremor (Xie et al., 2020). The region offshore Nicaragua hosted a M_w 7.7 earthquake that generated a tsunami in 1992, causing considerable damage whereas the 2012 M_w 7.6 offshore the Nicoya Peninsula did not generate any tsunamis (Satake, 1994; Norabuena et al., 2004; Dixon et al., 2014; Protti et al., 2014). The megathrust offshore Nicaragua also experiences many more moderate sized earthquakes compared to Nicoya (Figure 2), suggesting contrasts in frictional behavior between these two regions. In this paper, we use available geodetic data and a kinematic coupling model with a stress constraint to investigate the possibility of shallow, up-dip locking in these regions. For the Nicoya Peninsula of northern Costa Rica, with relatively dense geodetic coverage, we estimate a strain budget for the megathrust incorporating strain release via SSEs, and discuss implications for tsunami hazard assessment. Previous work indicates that the coupled regions offshore Nicoya extend to at least 10 km depth (Protti et al., 2014), but our models suggest that the coupled region extends to at least 5 km depth and potentially up to the trench.

2 GPS Data

In northern Costa Rica, we use the data from Xie et al. (2020) to compute interseismic and inter-SSE velocities for the periods before and after the M_w 7.6 5 September 2012 earthquake. The catalog spans July 2002 to July 2020 and contains ten cycles of SSEs. Pre- and post-earthquake locking patterns are remarkably similar, but the post-earthquake period has more stations.

In Nicaragua, we use GPS data processed by the University of Nevada, Reno (Blewitt et al., 2018), and model the GPS time series in the same way as the Costa Rican network, a linear regression with annual/semiannual signals and step-functions for station changes and earthquakes. Some of these stations are located on volcanoes and their signals may be contaminated by local volcanic effects. Several stations have short time spans ($\sim$1.5 years) and have large uncertainties on the interseismic velocities. One station, CN22, is located in a residential area of the coastal town of Poneloya, Nicaragua and displays mostly western motion, possibly indicating contamination by other sources of deformation.

Both the Costa Rican and Nicaraguan site velocity data exhibit significant northwest components associated with trench-parallel forearc block motion (Figure 3) (McCaffrey et al., 2002; DeMets, 2001; Norabuena et al., 2004; Turner et al., 2007; LaFemina et al., 2009). For the velocity of the subducted plate, we used the PVEL model (DeMets et al., 2010). Misfits between the predictions of this model and the observed GPS velocity at

Cocos Island (Protti et al., 2012) suggest that PVEL may be slightly biased, but the differences are not significant for purposes of our model. Since both Nicoya and southern Nicaragua experience motion of a forearc sliver block, we calculated the effective rake direction and rate on the subduction interface assuming 10 mm/yr of northwest block motion for Nicoya, and 15 mm/yr of northwest block motion for southern Nicaragua. The corresponding rake direction differs little from the predicted PVEL direction of motion, hence simply taking the component of motion for a given site velocity in the PVEL direction is an adequate approximation.

3 Kinematic Coupling Models offshore Northern Costa Rica

We divide the megathrust into discrete triangular patches following the Slab 2.0 plate interface (Hayes et al., 2018) and apply a new kinematic coupling model with stress-constraints on the fault patches (Lindsey et al., 2021). This model uses a boundary element method to apply analytical solutions for displacements and stressing rate in an elastic half space. The model imposes a non-zero stressing rate via the stress interaction kernel that acts as a physics-based minimum smoothness constraint. This stress kernel is constructed by evaluating the effect of the slip vector on each patch for all the patches. Thus, the smoothing effect of the stress-constraint is highest for regions that are up-dip of highly coupled patches. There is an additional Laplacian smoothing parameter within the model that does not exploit physics for a more variable smoothing effect. For that parameter, we use an L-curve approach and compute the point of maximum curvature to select an optimal smoothing parameter.

We used two types of priors (maximum and minimum coupling) to estimate the range of possible coupling behavior for the Central American megathrust. The priors are implemented by imposing a penalty on the total slip rate deficit. This is calculated by summing the slip rates on all the patches and penalizing the difference between that sum and either zero (minimum coupling) or the long-term slip rate (maximum coupling). The inversion is iterated over a range of reasonable penalty parameters for both the minimum and maximum solution, which allows tracking of the minimum and maximum allowable coupling values on each patch. The variance in the physical domain is defined by the difference between the maximum and minimum coupling values at each patch, and we use this as a metric for model resolution as well as computing model uncertainty. When the penalty parameter is zero there is no difference between the maximum and minimum solutions; this is the best-fitting model.

Our preferred model uses the interseismic velocities from the post-2012 period (Figure 4a). Regardless of the penalty parameter, all models show a highly coupled patch underneath the center of the Nicoya Peninsula and another highly coupled patch to the east beneath the Gulf of Nicoya. Increasing the penalty parameter on the minimum coupling inversion reduces the coupling around these two high-coupled patches and eventually, with a large enough parameter, the two main patches converge into one patch beneath the southeastern region of Nicoya. Conversely, increasing the penalty parameter on the maximum coupling inversion reduces the degree of coupling around these patches forcing increased coupling away from the data. The minimum coupling inversions tend to fit the data better than the maximum coupling inversions (i.e. the same penalty parameter yields a better fit in the minimum inversion compared to the maximum).

We also investigated interseismic velocities from the pre-2012 period. There is significant overlap in the coupling patches of both periods (Figure 4). For the pre-2012 model, the central patch is located farther offshore, and shows a highly-coupled region at about 35 km depth in the northwest region of Nicoya, consistent with modeled slow slip in 2009, 2011, and 2014 (Xie et al., 2020). Both models show strong correlation with the rupture zone of the 2012 Costa Rica earthquake (Figure 1 and 2), as well as deep slow slip ($\sim$40 km) beneath the Gulf of Nicoya.

All of the models (pre- and post-2012) indicate a high degree of variance in the near-trench portion of the subduction zone, with the maximum coupling close to the full plate rate. Figure 5 shows the minimum and maximum coupling on each patch over the range of solutions for the post-2012 period and a transect perpendicular to the trench. The coupling is well-constrained in the region of the 2012 rupture zone between 40−70% with the best-fit values being between 50−60% coupled for both the pre- and post-2012 periods. Figure 5c also compares the coupling values to strain release processes associated with this section of the megathrust (coseismic ruptures, postseismic slip, and SSEs). Large earthquakes and SSEs apparently release most of the accumulated strain in the deeper parts of the subduction zone, but do not fully accommodate the shallow strain. At the trench, the variability ranges from a minimum of 15% up to $\sim 98\%$, effectively full coupling. This variability is also seen in adjacent sections of the trench (Figure 6).

4 Forward Locking Models offshore Southern Nicaragua

The GPS network in Nicaragua is not sufficiently dense nor close enough to the trench to apply the coupling model reliably. However, with some assumptions, useful information about the frictional behavior of the megathrust can be obtained from simple forward models. We tested whether the tsunami or seismological/aftershock models of the 1992 M_w 7.7 earthquake are consistent with the available GPS data, assuming that the rupture zone for that event is also the zone that is currently fully locked.

We modeled the interseismic velocities in Nicaragua with a range of locking models in the shallow megathrust (Okada, 1992). Seismological models, based on aftershock distribution, tend to favor large rupture zones with significant down-dip extent (Ide et al., 1993; Norabuena et al., 2004). These models are not consistent with the current GPS velocity field. Figure 7 shows a range of locking models and the tsunami rupture model of Satake (1994). The GPS locking model and the tsunami rupture model both imply a limited depth down-dip extent of locking/rupture, $\sim\ 40 - 50$ km, at a depth of approximately $20 - 25$ km on the plate interface.

5 Discussion

The tsunami record in Costa Rica dates back to 1579 and includes 14 events related to earthquakes (NOAA, 2020). The tsunami associated with the M_w 7.6 1991 Limón earthquake is the only significant event recorded with wave heights of $\sim 2-3$ m. However, this earthquake and tsunami occurred on the Caribbean side of Costa Rica and are unrelated to the subduction megathrust. All other tsunamis in Costa Rica have been small, with $10 - 30$ cm wave heights.

The megathrust offshore the Nicoya Peninsula in northwest Costa Rica hosts earthquakes of order M_w 7.5 with a recurrence interval of 50−60 years (Protti et al., 2014), but there are no recorded tsunamis associated with these events. In contrast, areas in Central America northwest of Costa Rica do host significant tsunamis. In 1992, a M_w 7.7 earthquake offshore Nicaragua generated a tsunami with ~ 10 m waves that killed at least 168 people and left 13,500 homeless (Kanamori & Kikuchi, 1993; Satake, 1994; Kikuchi & Kanamori, 1995; Satake, 1995). In 2003, a M_w 7.3 megathrust earthquake in El Salvador near the Gulf of Fonseca created a tsunami with ∼6.3 m wave heights (Heidarzadeh & Satake, 2014).

The contrast in recent and historical tsunami behavior between these two adjacent sections of the Central American subduction zone raises an obvious question. Are large tsunamis offshore Costa Rica not possible, or is the tsunami/earthquake record simply too short to have observed these events? In other words, is there a fundamental difference in the properties of the subduction megathrust that limits tsunami risk offshore Costa Rica, versus megathrust properties to the north that promote tsunamis?

The record length for Costa Rica (∼450 year) is long enough to suggest the difference in tsunami recurrence between two areas is significant. Perhaps the absence of tsunamis in Costa Rica reflects a lack of strain accumulation in the shallow megathrust here; data from the current on-shore geodetic network are not diagnostic as they lacks sensitivity to strain accumulation near the trench. Our new kinematic strain accumulation model, accounting for realistic stress shadow effects, provide some constraints and suggests that strain may indeed be accumulating in this up-dip region but uncertainties remain large. Jiang et al. (2017) documented an elastic strain release event in the shallow megathrust offshore Nicoya, suggesting prior strain accumulation here.

If up-dip strain had indeed accumulated here, why was it not released in the 2012 earthquake? Recent models of earthquake 'super-cycles' suggest that strain can accumulate over many earthquake cycles, i.e. all accumulated strain is not necessarily released in a given event (Sieh et al., 2008; Salditch et al., 2020). It has also been shown that large earthquakes tend to cluster in time (Kulkarni et al., 2013; Goldfinger et al., 2013), consistent with the idea of temporal variation of strain accumulation/release. If these concepts apply to Costa Rica, it is possible that long-term strain is accumulating near the trench and could contribute to a large tsunami in the future.

The coupling model from Protti et al. (2014) suggests that there is a fully coupled area along the coast of the Nicoya Peninsula that did not rupture during the 2012 earthquake. Our models suggest that this region is $\sim 40\%$ coupled and accruing $\sim 3{-}3.5\,\mathrm{cm/yr}$ of slip. This region also experiences SSEs approximately every two years and releases about $1.5{-}2\,\mathrm{cm}$ of strain (Voss et al., 2017; Xie et al., 2020; Afra et al., submitted to JGR). This suggests that this area may be accumulating strain more slowly than previously thought and perhaps explains why it did not participate in the 2012 rupture, though this does not preclude it from participating in future great earthquakes.

The slip rate deficit at the trench estimated by our models is between $10 - 95\%$ of the plate rate ($\sim 0.85{-}8.5\,\mathrm{cm/yr}$) (Figure 5c). Hence, the potential strain accumulation offshore Costa Rica is of order $\sim 4{-}35\,\mathrm{m}$ based on the 450 year record of no tsunamis. While this maximum value seems extreme, we note that even higher strain release was observed in Japan during the 2011 M_w 9.0 Tohoku-Oki earthquake. Prior to that event, the up-dip region of the seismogenic zone had been considered aseismic (velocity strengthening), incapable of hosting rapid seismic slip. In the event, the earthquake caused up to $\sim$50 m of offset at the trench (Kimura et al., 2012). Before the 2011 Tohoku-Oki event, the megathrust had a prior history of recurring M $\sim$ 7 earthquakes (1915, 1962, 1980, 2003) (Uchida & Bürgmann, 2021). The potential similarity with the Costa Rican record suggests to us that tsunami hazard estimates in this part of Central America based only on the historical record could be under-estimated, despite that record's 450-year length.

The forward locking models offshore Southern Nicaragua are consistent with the tsunami model proposed by Satake (1994), but due to the uncertainties on the interseismic velocities it is difficult to estimate anything more than the down-dip extent of locking. The down-dip extent is consistent with shallow locking and our models rule out deep locking offshore Nicaragua (Figure 8). Sea-floor geodetic data would help to better constrain the down-dip extent and more localized regions of locking.

Assuming the tsunami rupture model accurately outlines the current locking pattern, as suggested by the limited GPS data, there is a spatial correlation between locking and bathymetric depth. The steep gradient in near-trench bathymetry, from about 4,000 meters to less than 500 meters within 45 km of the trench, closely matches the region we infer to be presently locked. Perhaps this locked zone persists over many seismic cycles, promoting back-thrusts that locally steepen and thicken the crust. Xie et al. (2020) noted the similarity between pre- and post-2012 locking patterns in and near the Nicoya peninsula, also consistent with longer term persistence in locking patterns.

There were over 250 moderate earthquakes ($M_w 5-6.9$) between 1976 and 2022 offshore Southern Nicaragua and Northern Costa Rica (Figure 2). Prior to the 1992 event, seismicity is sparsely distributed offshore Nicaragua. After the 1992 event two major clusters of seismicity occur offshore Nicaragua, southeast and northwest of the hypocenter. These high-density clusters largely overlap with the locking zone inferred from the geodetic data.

Three normal-faulting earthquakes occurred in the outer-rise in the year after the 1992 Nicaragua earthquake. These types of earthquakes have been interpreted to indicate prior shallow locking, with the subsequent large megathrust earthquake stimulating extension in the outer-rise (Sladen & Trevisan, 2018). Offshore Nicoya there are not as many clear indicators of shallow locking such as the high-volume of earthquakes near the trench or large tsunami run-ups. Though there are fewer outer-rise earthquakes, there are two prior to the 2012 earthquake and one after 2013, all greater than M_w 5.0.

The available tsunami, seismic, and geodetic data in Nicaragua are in agreement that the near-trench region is locked and can generate tsunamis. Assuming locking continues, at the full plate rate, this portion of the subduction zone will reach 3 meters of accumulated strain (the amount released in the 1992 earthquake) within the next $1-3$ decades.

6 Conclusions

- A stress-constrained kinematic coupling model for the interseismic surface velocity field in northern Costa Rica predicts a locked (slip deficit) zone that agrees with the rupture zone of the 2012 M_w 7.6 Costa Rica earthquake. The model suggests the offshore region experiences slip deficit at $10-95\%$ of the full plate rate, with 25% as the best estimate. The potential therefore exists for a major tsunami here, despite a 450-year tsunami-free record.
- The GPS surface velocity field in Nicaragua is consistent with a shallow locking model that resembles the 1992 tsunami rupture model of Satake (1994).
- If the shallow megathrust offshore Nicaragua remains fully locked, as implied by the limited GPS data, there is potential for another large earthquake and tsunami within the next 1-3 decades.
- Sea-floor geodesy would significantly improve our ability to constrain locking on the shallow megathrust in both Nicaragua and Costa Rica.

7 Acknowledgments

This research was partially supported by the National Science Foundation grants 1835947 to T. H. D. Special thanks to Emile Okal for referring us to the NOAA tsunami database. We would also like to thank Jochen Braunmiller for reviewing and challenging our models throughout the process.

References

Afra, M., Hastings, M. S., Xie, S., Chaves, E., Muller, C., Protti, M., ... Alvarez-Calderón, A. (submitted to JGR). Slow slip prior to an earthquake: An example from costa rica and forecasting implications. *Journal of Geophysical Research: Solid Earth*.

Blewitt, G., Hammond, W. C., & Kreemer, C. (2018). Harnessing the gps data explosion for interdisciplinary science. *Eos*, *99*(10.1029), 485.

Bürgmann, R., & Chadwell, D. (2014). Seafloor geodesy. *Annual Review of Earth and Planetary Sciences*, *42*, 509–534.

DeMets, C. (2001). A new estimate for present-day cocos-caribbean plate motion: Implications for slip along the central american volcanic arc. *Geophysical research letters*, *28*(21), 4043–4046.

DeMets, C., Gordon, R. G., & Argus, D. F. (2010). Geologically current plate motions. *Geophysical journal international*, *181*(1), 1–80.

Dixon, T. H., Jiang, Y., Malservisi, R., McCaffrey, R., Voss, N., Protti, M., & Gonzalez, V. (2014). Earthquake and tsunami forecasts: Relation of slow slip events to subsequent earthquake rupture. *Proceedings of the National Academy of Sciences*, *111*(48), 17039–17044.

Dziewonski, A. M., Chou, T.-A., & Woodhouse, J. H. (1981). Determination of earthquake source parameters from waveform data for studies of global and regional seismicity. *Journal of Geophysical Research: Solid Earth*, *86*(B4), 2825–2852.

Goldfinger, C., Ikeda, Y., Yeats, R. S., & Ren, J. (2013). Superquakes and supercycles. *Seismological Research Letters*, *84*(1), 24–32.

Hayes, G. P., Moore, G. L., Portner, D. E., Hearne, M., Flamme, H., Furtney, M., & Smoczyk, G. M. (2018). Slab2, a comprehensive subduction zone geometry model. *Science*, *362*(6410), 58–61.

Heidarzadeh, M., & Satake, K. (2014). The el salvador and philippines tsunamis of august 2012: insights from sea level data analysis and numerical modeling. *Pure and Applied Geophysics*, *171*(12), 3437–3455.

Ide, S., Imamura, F., Yoshida, Y., & Abe, K. (1993). Source characteristics of the nicaraguan tsunami earthquake of september 2, 1992. *Geophysical research letters*, *20*(9), 863–866.

Jiang, Y., Liu, Z., Davis, E. E., Schwartz, S. Y., Dixon, T. H., Voss, N., ... Protti, M. (2017). Strain release at the trench during shallow slow slip: The example of nicoya peninsula, costa rica. *Geophysical Research Letters*, *44*(10), 4846–4854.

Kanamori, H., & Kikuchi, M. (1993). The 1992 nicaragua earthquake: a slow tsunami earthquake associated with subducted sediments. *Nature*, *361*(6414), 714–716.

Kikuchi, M., & Kanamori, H. (1995). Source characteristics of the 1992 nicaragua tsunami earthquake inferred from teleseismic body waves. In *Tsunamis: 1992–1994* (pp. 441–453). Springer.

Kimura, G., Hina, S., Hamada, Y., Kameda, J., Tsuji, T., Kinoshita, M., & Yamaguchi, A. (2012). Runaway slip to the trench due to rupture of highly pressurized megathrust beneath the middle trench slope: the tsunamigenesis of the 2011 tohoku earthquake off the east coast of northern japan. *Earth and Planetary Science Letters*, *339*, 32–45.

Kulkarni, R., Wong, I., Zachariasen, J., Goldfinger, C., & Lawrence, M. (2013). Statistical analyses of great earthquake recurrence along the cascadia subduction zone. *Bulletin of the Seismological Society of America*, *103*(6), 3205–3221.

LaFemina, P., Dixon, T. H., Govers, R., Norabuena, E., Turner, H., Saballos, A., ... Strauch, W. (2009). Fore-arc motion and cocos ridge collision in central america. *Geochemistry, Geophysics, Geosystems*, *10*(5).

Li, S., Wang, K., Wang, Y., Jiang, Y., & Dosso, S. E. (2018). Geodetically inferred locking state of the cascadia megathrust based on a viscoelastic earth model. *Journal of Geophysical Research: Solid Earth*, *123*(9), 8056–8072.

Lindsey, E. O., Mallick, R., Hubbard, J. A., Bradley, K. E., Almeida, R. V., Moore, J. D., ... Hill, E. M. (2021). Slip rate deficit and earthquake potential on shallow megathrusts. *Nature Geoscience*, *14*(5), 321–326.

McCaffrey, R., Stein, S., & Freymueller, J. (2002). Crustal block rotations and plate coupling. *Plate Boundary Zones, Geodyn. Ser*, *30*, 101–122.

NOAA. (2020). National geophysical data center/world data service: Ncei/wds global historical tsunami database.

Norabuena, E., Dixon, T. H., Schwartz, S., DeShon, H., Newman, A., Protti, M., ... others (2004). Geodetic and seismic constraints on some seismogenic zone processes in costa rica. *Journal of Geophysical Research: Solid Earth*, *109*(B11).

Okada, Y. (1992). Internal deformation due to shear and tensile faults in a half-space. *Bulletin of the seismological society of America*, *82*(2), 1018–1040.

Protti, M., González, V., Freymueller, J., & Doelger, S. (2012). Isla del coco, on cocos plate, converges with isla de san andrés, on the caribbean plate, at 78mm/yr. *Revista de Biología Tropical*, *60*, 33–41.

Protti, M., González, V., Newman, A. V., Dixon, T. H., Schwartz, S. Y., Marshall, J. S., ... Owen, S. E. (2014). Nicoya earthquake rupture anticipated by geodetic measurement of the locked plate interface. *Nature Geoscience*, *7*(2), 117–121.

Protti, M., McNally, K., Pacheco, J., Gonzalez, V., Montero, C., Segura, J., ... others (1995). The march 25, 1990 (mw= 7.0, ml= 6.8), earthquake at the entrance of the nicoya gulf, costa rica: Its prior activity, foreshocks, aftershocks, and triggered seismicity. *Journal of Geophysical Research: Solid Earth*, *100*(B10), 20345–20358.

Salditch, L., Stein, S., Neely, J., Spencer, B. D., Brooks, E. M., Agnon, A., & Liu, M. (2020). Earthquake supercycles and long-term fault memory. *Tectonophysics*, *774*, 228289.

Satake, K. (1994). Mechanism of the 1992 nicaragua tsunami earthquake. *Geophysical Research Letters*, *21*(23), 2519–2522.

Satake, K. (1995). Linear and nonlinear computations of the 1992 nicaragua earthquake tsunami. *Pure and Applied Geophysics*, *144*(3), 455–470.

Schmalzle, G. M., McCaffrey, R., & Creager, K. C. (2014). Central cascadia subduction zone creep. *Geochemistry, Geophysics, Geosystems*, *15*(4), 1515–1532.

Sieh, K., Natawidjaja, D. H., Meltzner, A. J., Shen, C.-C., Cheng, H., Li, K.-S., ... Edwards, R. L. (2008). Earthquake supercycles inferred from sea-level changes recorded in the corals of west sumatra. *Science*, *322*(5908), 1674–1678.

Sladen, A., & Trevisan, J. (2018). Shallow megathrust earthquake ruptures betrayed by their outer-trench aftershocks signature. *Earth and Planetary Science Letters*, *483*, 105–113.

Turner, H. L., LaFemina, P., Saballos, A., Mattioli, G. S., Jansma, P. E., & Dixon, T. (2007). Kinematics of the nicaraguan forearc from gps geodesy. *Geophysical Research Letters*, *34*(2).

Uchida, N., & Bürgmann, R. (2021). A decade of lessons learned from the 2011 tohoku-oki earthquake. *Reviews of Geophysics*, *59*(2), e2020RG000713.

Voss, N. K., Malservisi, R., Dixon, T. H., & Protti, M. (2017). Slow slip events in the early part of the earthquake cycle. *Journal of Geophysical Research: Solid Earth*, *122*(8), 6773–6786.

Wallace, L. M., Webb, S. C., Ito, Y., Mochizuki, K., Hino, R., Henrys, S., ... Sheehan, A. F. (2016). Slow slip near the trench at the hikurangi subduction zone, new zealand. *Science*, *352*(6286), 701–704.

Xie, S., Dixon, T. H., Malservisi, R., Jiang, Y., Protti, M., & Muller, C. (2020).

Slow slip and inter-transient locking on the nicoya megathrust in the late and early stages of an earthquake cycle. *Journal of Geophysical Research: Solid Earth*, *125*(11), e2020JB020503.

Yokota, Y., Ishikawa, T., Watanabe, S.-i., Tashiro, T., & Asada, A. (2016). Seafloor geodetic constraints on interplate coupling of the nankai trough megathrust zone. *Nature*, *534*(7607), 374–377.

Yue, H., Lay, T., Schwartz, S. Y., Rivera, L., Protti, M., Dixon, T. H., ... Newman, A. V. (2013). The 5 september 2012 nicoya, costa rica mw 7.6 earthquake rupture process from joint inversion of high-rate gps, strong-motion, and teleseismic p wave data and its relationship to adjacent plate boundary interface properties. *Journal of Geophysical Research: Solid Earth*, *118*(10), 5453–5466.

396 # 8 Figures

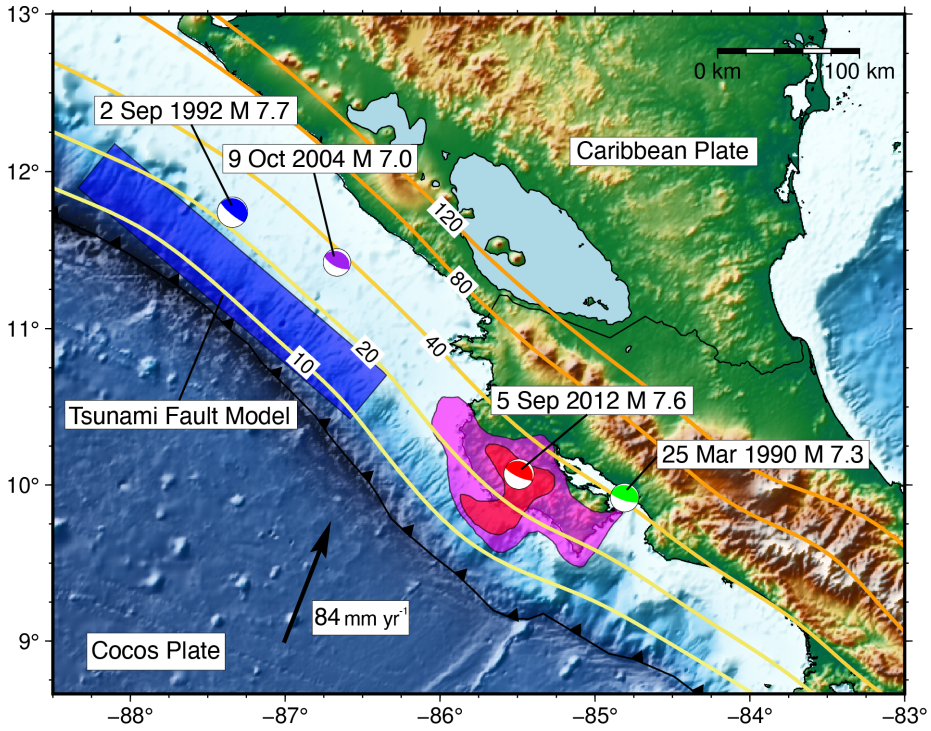

Figure 1. Bathymetry and topography of the study area based on a 30-arc second Digital Elevation Model of Central America, with major earthquakes (USGS) and selected depth contours (in km) on the subducting plate interface. Rupture zone of the 2012 M_w 7.6 Costa Rica earthquake (red patch is the 1.2 meter slip contour of Yue et al. (2013)) and pre-seismic locked zone for the event (magenta patch is the area with coupling ratio greater than 0.3 in coupling model of Protti et al. (2014)) are shown for comparison. Rupture zone of the 1992 M_w 7.7 Nicaragua earthquake (blue rectangle) is inferred from the tsunami fault model of Satake (1994).

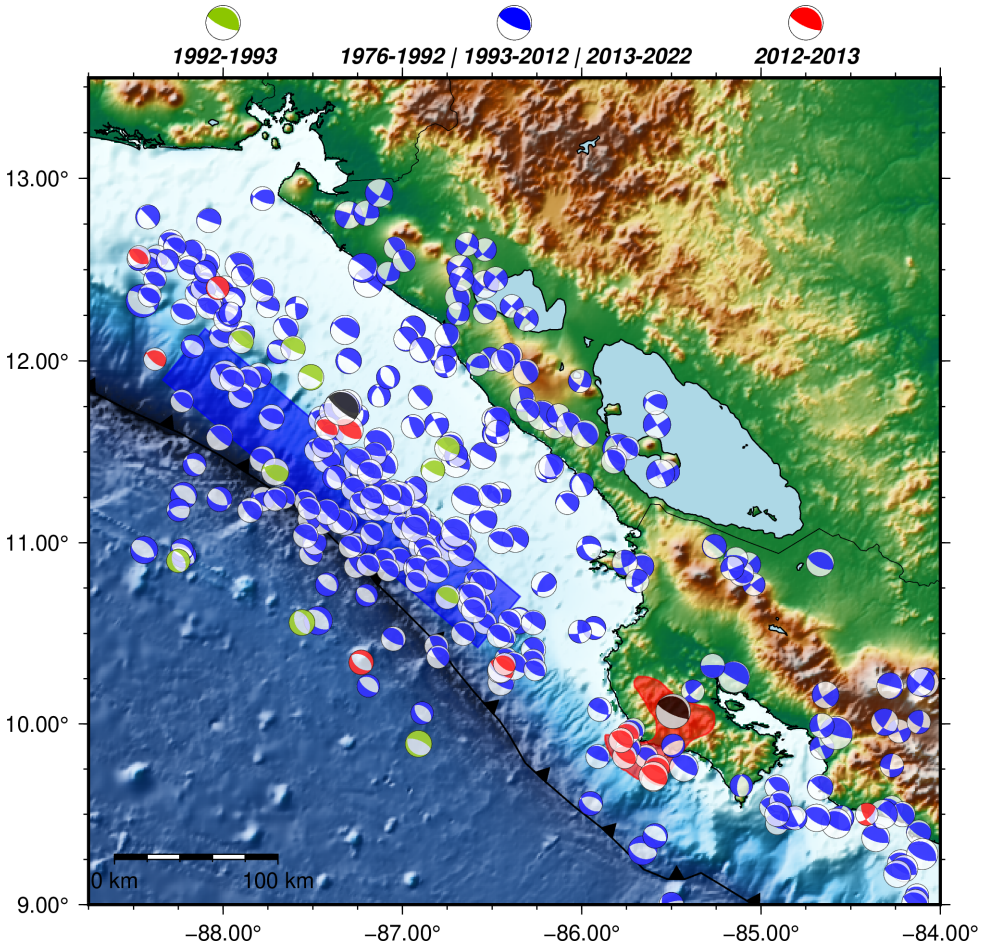

Figure 2. Comparison of earthquake frequency and location offshore northern Costa Rica and Nicaragua, from the Global Centroid Moment Tensor Catalog (Dziewonski et al., 1981). One year aftershocks from the 1992 M_w 7.7 Nicaragua and 2012 M_w 7.6 Costa Rica earthquakes are color-coded, light green and red, respectively.

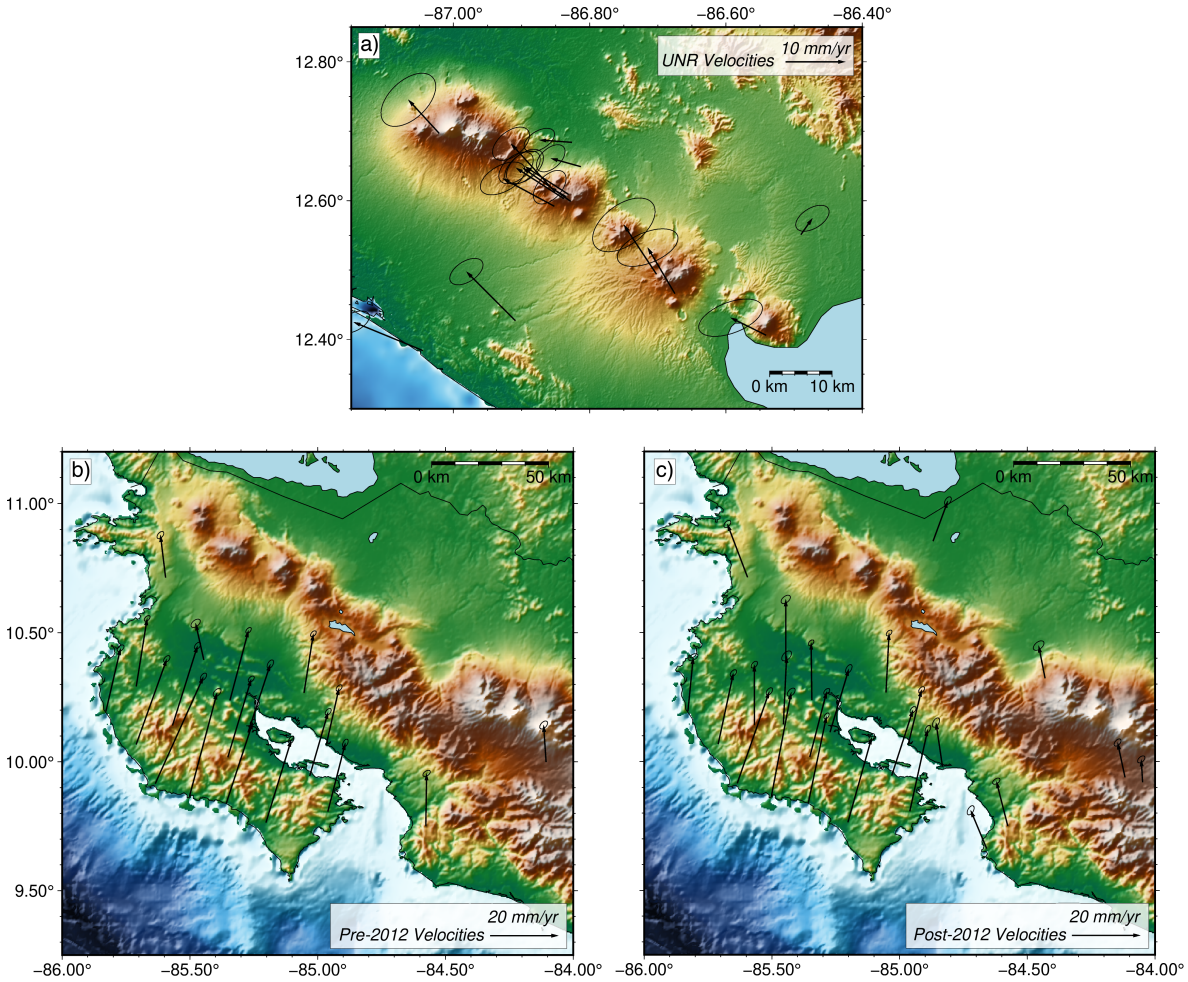

Figure 3. Interseismic surface velocity for (a) Nicaragua (Blewitt et al., 2018) and (b,c) Costa Rica (Xie et al., 2020). Costa Rica data show periods before and after the 2012 M_w 7.6 earthquake. Both periods have similar velocity patterns, reflecting a combination of plate motion-parallel strain accumulation from locking on the megathrust and trench-parallel forearc motion. Nicaragua data, farther from the locked megathrust, are dominated by trench-parallel forearc motion.

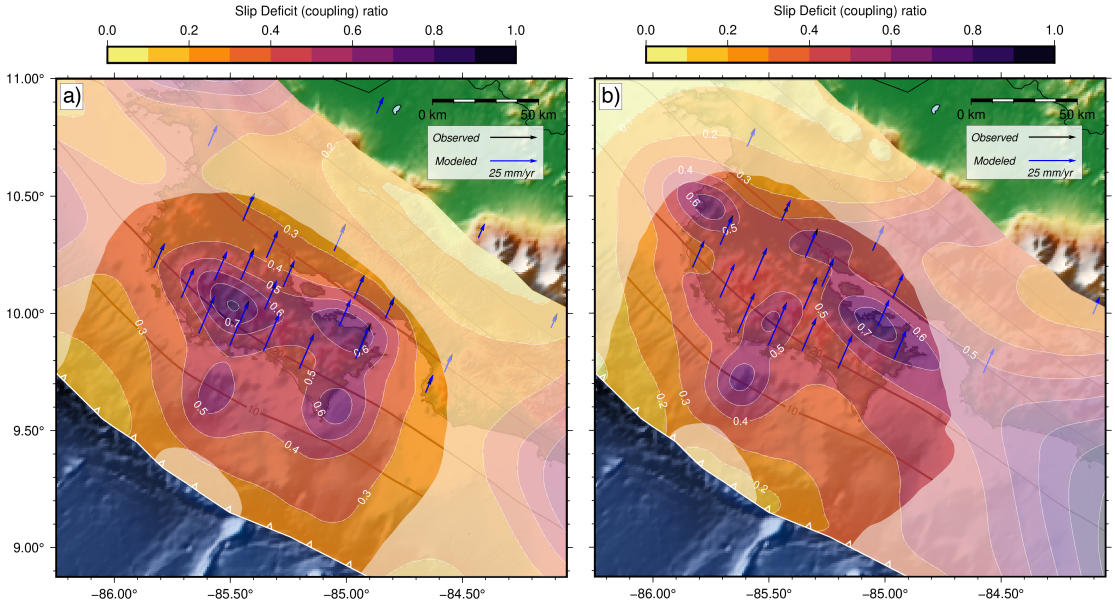

Figure 4. (a) Best-fit kinematic coupling model for northern Costa Rica using plate motion-parallel component of interseismic surface velocities (black arrows are data vectors and blue are model vectors) for the the post-2012 period and the (b) pre-2012 period. The models are overlain on a regional DEM, with more transparent sections indicating poorly constrained regions (see Figure 6). Thin black contours show slab depth from Hayes et al. (2018).

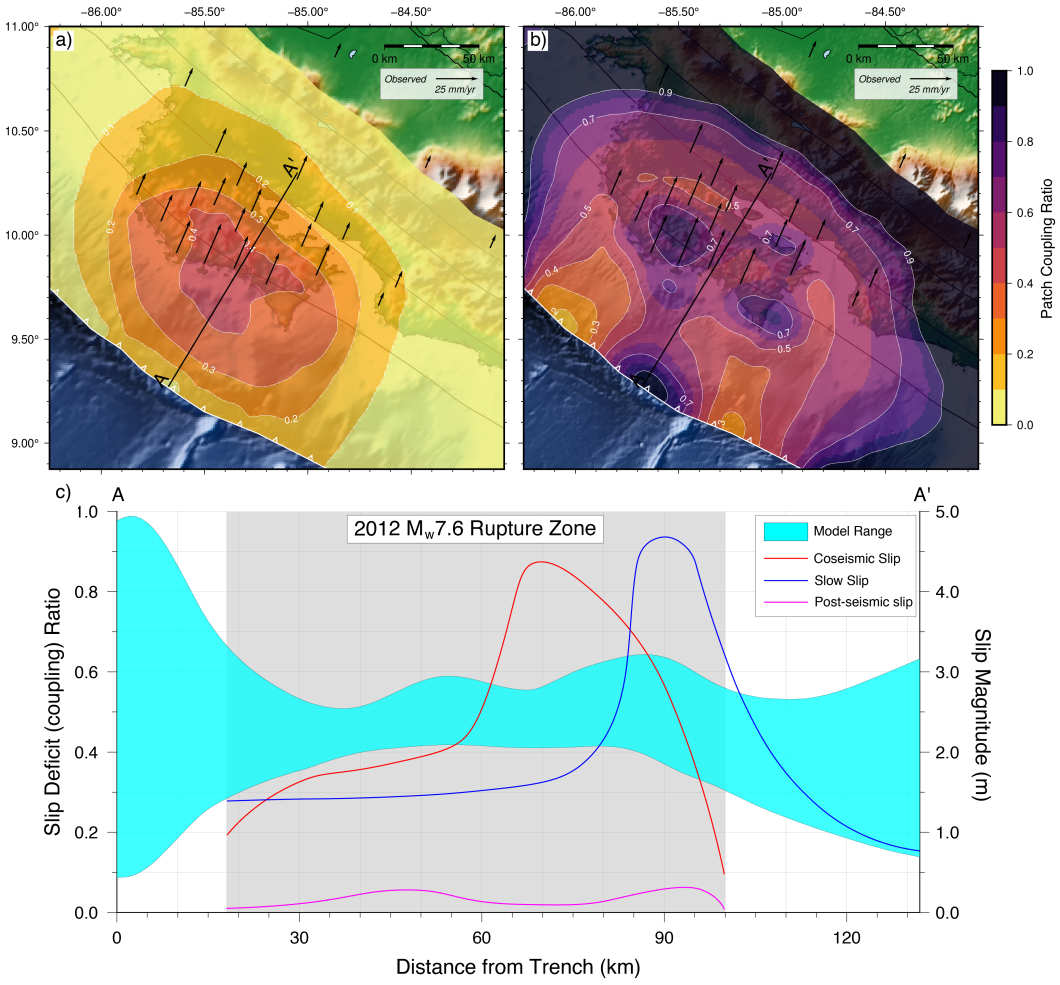

Figure 5. Minimum (a) and maximum (b) coupling ratio for each patch (location) from a range of inversion solutions. Line A-A' shows the location of the trench-perpendicular transect through the rupture zone of the 2012 M_w 7.6 earthquake. (c) Comparison of strain accumulation (slip deficit) along line A-A' and various strain release processes (earthquake rupture, post-seismic slip, and slow slip). Note that a significant fraction of accumulated strain may be unreleased in the offshore region close to the trench, implying that the possibility of a future tsunami, but uncertainties are large due to lack of near-trench observations.

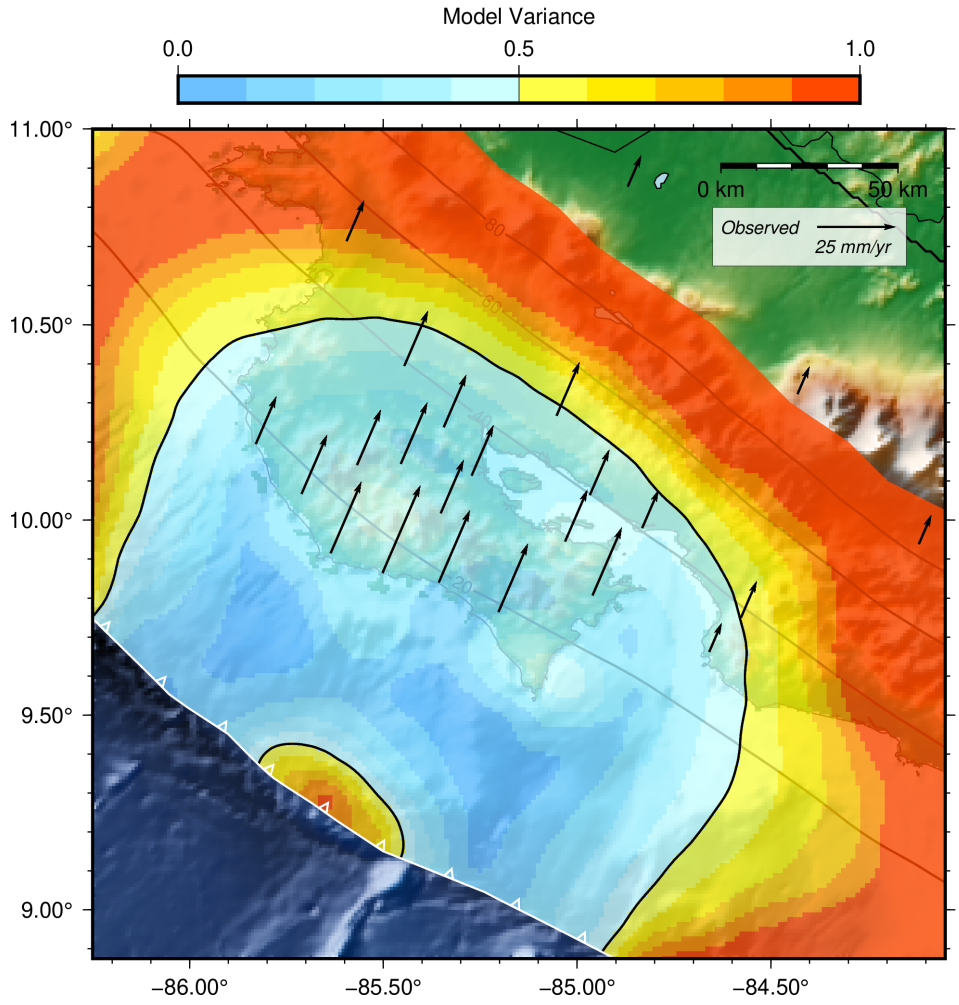

Figure 6. Variance in the coupling ratio for each patch in the model. Values larger than 0.5 are poorly constrained.

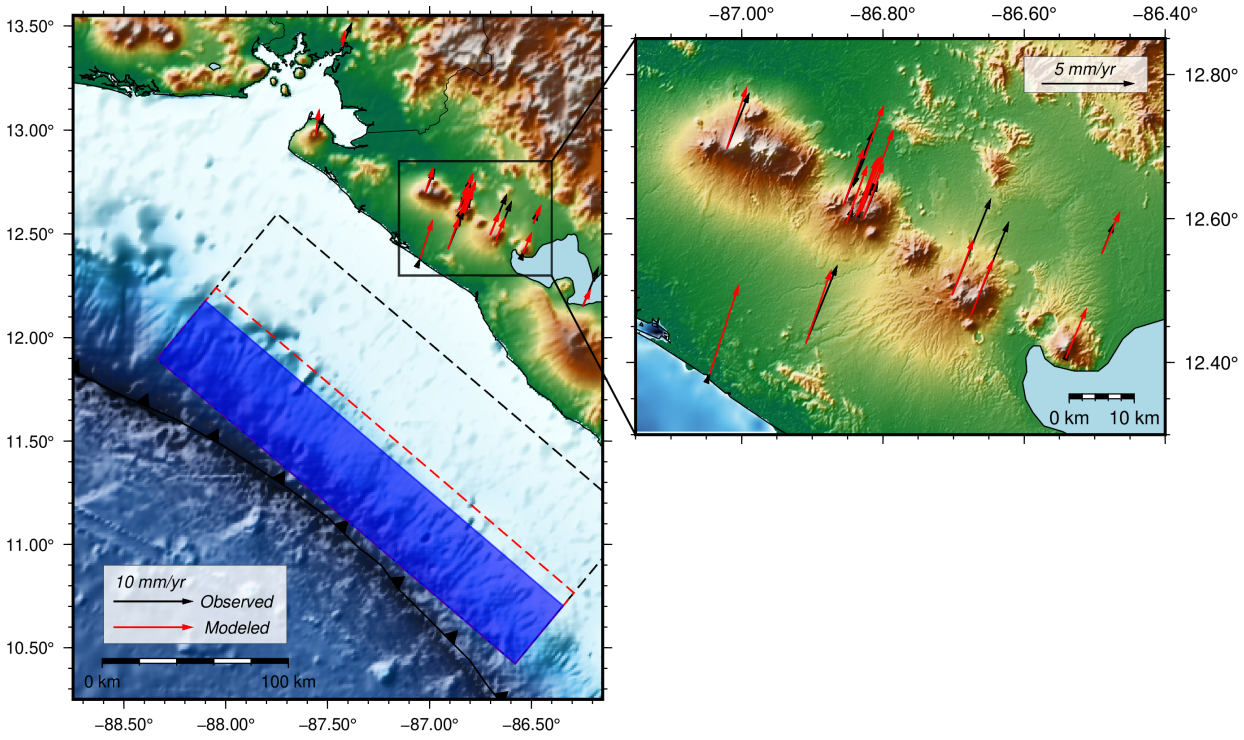

Figure 7. Proposed rupture models for the 1992 M_w 7.7 Nicaragua earthquake based on aftershock distribution (dashed black rectangle; Ide et al. (1993)) and tsunami run-up (blue solid rectangle; Satake (1994)), compared to a GPS-based forward model for locking (red dashed line). Inset shows GPS surface velocity data (black arrows) and predictions from the best-fit forward model (red arrows), which closely matches the tsunami-based rupture model.

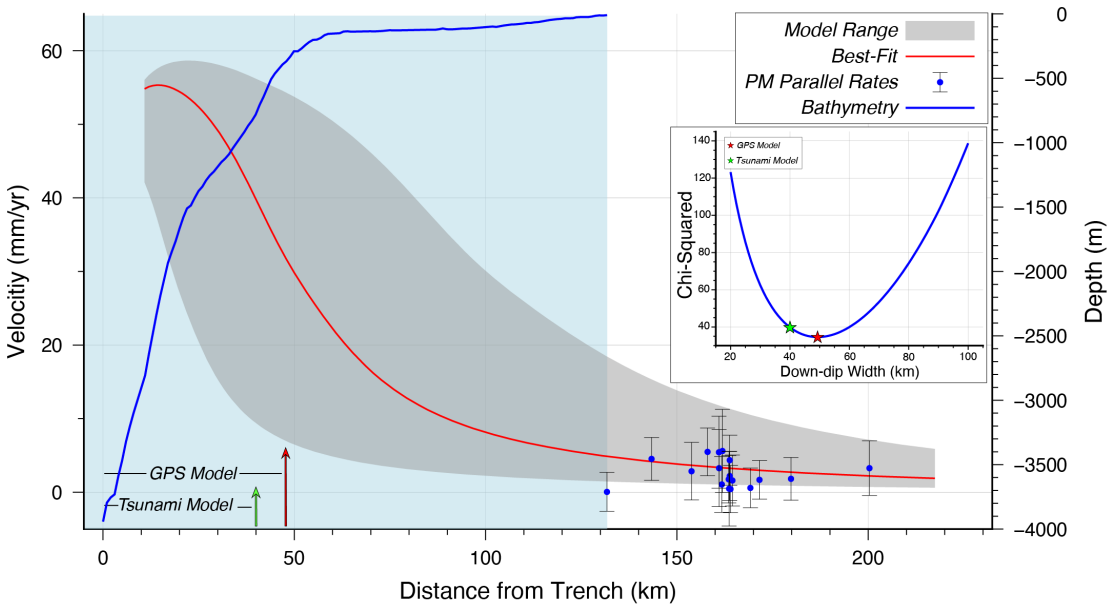

Figure 8. Bathymetric profile offshore Nicaragua compared to surface velocities predicted by the GPS-based locking model in Figure 7. Inset shows the chi-squared error for various depths of maximum locking in the forward model. Note the close agreement between the GPS locking model and the tsunami rupture model. While the on-shore GPS data are far from the locked zone, they can at least rule out the deeper down-dip width implied by the seismological model in Figure 7 assuming current locking matches the 1992 rupture.